The geometry and statistics of mixing in aperiodic flows

A. C. Poje and G. Haller
Division of Applied Mathematics, Brown University, Providence, Rhode Island 02912

I. Mezić
Department of Mechanical and Environmental Engineering and Department of Mathematics,
University of California, Santa Barbara, California 93106-5070

The relationship between statistical and geometric properties of particle motion in aperiodic, two-dimensional flows is examined. Finite-time-invariant manifolds associated with transient hyperbolic trajectories are shown to divide the flow into distinct regions with similar statistical behavior. In particular, numerical simulations of simple, eddy-resolving barotropic flows indicate that there exists a close correlation between such geometric structures and *patchiness* plots that describe the distribution of Lagrangian average velocity over initial conditions. For barotropic turbulence, we find that Eulerian velocity correlation time scales are significantly longer than their Lagrangian counterparts indicating the existence of well-defined Lagrangian structures. Identification of such structures shows a similar, close relationship between the invariant manifold geometry and patchiness calculations at intermediate time scales, where anomalous dispersion rates are found. © *1999 American Institute of Physics.* [S1070-6631(99)02910-4]

I. INTRODUCTION

The dynamical systems perspective on the problem of mixing in fluid flows was introduced in the paper of Aref,[1] where particle motion in a two-dimensional point-vortex-driven oscillatory flow was analyzed. Since then the subject has been treated in numerous papers (see, e.g., Ottino[2] for a survey). While the dynamical analysis of mixing in two-dimensional time-periodic and quasiperiodic flows has received much attention, mixing mechanisms in aperiodic flows have mainly been treated using a combination of numerical and probabilistic tools (see, e.g., Babiano *et al.*,[3] del Castillo,[4] Weiss *et al.*,[5] Zaslavsky,[6] and Ziemniak *et al.*[7]). The main reason is that several key results in dynamical systems theory are formulated in terms of maps, and hence are inapplicable to flows whose evolution cannot be approximated via repeated iterations of a map. Another reason is that dynamical systems has traditionally been concerned with asymptotic behavior, a concept that is undefined for finite-time experimental and numerical datasets.

Recently, two different approaches have been proposed in dynamical systems to circumvent the difficulty of aperiodic time dependence. First, Mezić[8] used tools from ergodic theory to study and predict Lagrangian velocity averages in two-dimensional flows. Such averages can be used to construct *patchiness plots* that reveal regions in the flow with similar finite-time statistical properties (cf. Malhotra *et al.*[9]). Second, Haller and Poje[10] developed a geometric theory of mixing in two-dimensional, aperiodic fluid flows. This computer assisted analytic theory enables one to construct *finite-time* invariant manifolds for any finite-time velocity dataset, thereby providing a complete understanding of individual mixing events associated with mesoscale structures in applications (cf. Poje and Haller[11] and also Miller *et al.*[12]).

In this paper we explore the connection between finite-time mixing theory and patchiness plots for realizable, aperiodic flows. In Sec. II the geometric theory of mixing for aperiodic flows is reviewed. We recall how finite-time-invariant manifolds provide exact templates for particle dynamics and divide the flow into regions with similar mixing properties. In sec. III the notion of *patchiness plots* is introduced and shown to be a powerful diagnostic tool for aperiodic flows. A comparison of the two approaches and a discussion of their remarkable correlation is given in Sec. IV, where the phenomena of oceanographic eddy shedding and two-dimensional turbulence are treated by these techniques.

II. FINITE-TIME-INVARIANT MANIFOLDS AND MIXING

We consider a two-dimensional velocity field of the form

$$\dot{x} = u(x,y,t), \quad \dot{y} = v(x,y,t), \tag{1}$$

and assume that on the time interval $[t^-, t^+]$, the velocity field admits a set of closed velocity contours bounded by a time-dependent, singular contour curve ϕ_t that contains a saddle-type stagnation point $p(t) = [x(t), y(t)]$ [see Fig. 1(a)]. We refer to this structure as a *kinematic eddy*.

As shown in Haller and Poje,[10] if the deformation rate of the kinematic eddy stays below a theoretical bound, then the flow admits a nearby *hyperbolic fluid particle motion* $\Gamma(t) = [\Gamma_x(t), \Gamma_y(t)]$ that attracts a set $W^s(\Gamma)$ of initial conditions exponentially, and repels another set $W^u(\Gamma)$. These sets are two-dimensional surfaces in the extended phase space of the variables (x,y,t) and can be considered as finite-time analogs of the well-known stable and unstable manifolds of dynamical systems theory. However, unlike stable and unstable manifold, $W^s(\Gamma)$ and $W^u(\Gamma)$ are not unique, which is related to the fact that they are constructed based on finite-time information. Still, they turn out to be unique up to
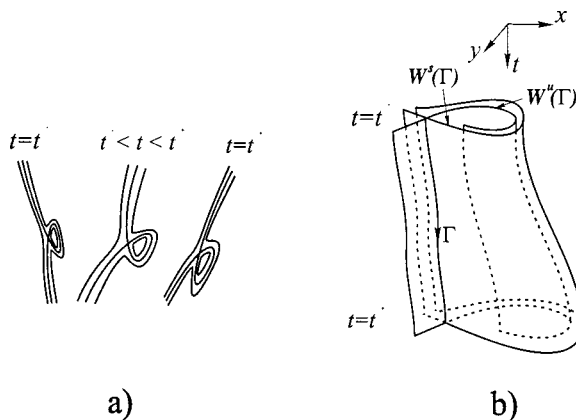
FIG. 1. (a) The formation of a *kinematic eddy* in the Eulerian field. (b) The *dynamic eddy* defined by stable and unstable sets in the extended phase space.

errors that vanish exponentially as either the time interval $\Delta t = t^+ - t^-$ or the strength of the hyperbolicity increases. In summary, if the speed and the deformation rate of a kinematic eddy are not too large, and if it exists on a long enough time interval, then a ''saddle-type'' fluid particle motion exists near the path spanned by the stagnation point $p(t)$, with *finite-time stable and unstable manifolds* that are uniquely determined for all practical purposes. Complete proofs of these statements as well as a sample application can be found in Haller and Poje.[10]

Once the existence of exponentially unique stable and unstable manifolds is known, they can be determined numerically using the straddling techniques developed in Miller *et al.*[12] The numerically determined manifolds $W^s(\Gamma)$ and $W^u(\Gamma)$, in turn, define the boundaries of a *dynamic eddy* in the extended phase space [see Fig. 1(b)]. They also provide an exact classification of initial conditions in terms of their finite-time behavior. Namely, fluid particles falling in the ''channel'' between the two manifold are mixed into the eddy, while all other particles are excluded from mixing. This enables one to define exact eddy boundaries in Lagrangian terms, complementing Eulerian definitions such as those given by Weiss.[13]

III. STATISTICAL PROPERTIES OF PARTICLE MOTION

In a bounded domain $\mathcal{M}$, let f be an arbitrary bounded function $f: \mathcal{M} \rightarrow \mathbb{R}$. The finite-time average of f along the particle paths of a two-dimensional velocity field $\mathbf{v}$, is given by

$$f^*(t, x_0, y_0) = \frac{1}{t} \int_0^t f[x(\tau, x_0, y_0), y(\tau, x_0, y_0), \tau] d\tau, \quad (2)$$

where $x(\tau, x_0)$ is the location, at time $t = \tau$, of a particle located at x_0 at time $t = 0$. For a velocity field with periodic time dependence, it can be shown (see Mezić,[8] Mezić and Wiggins[14]) that in the infinite-time limit the level sets of the
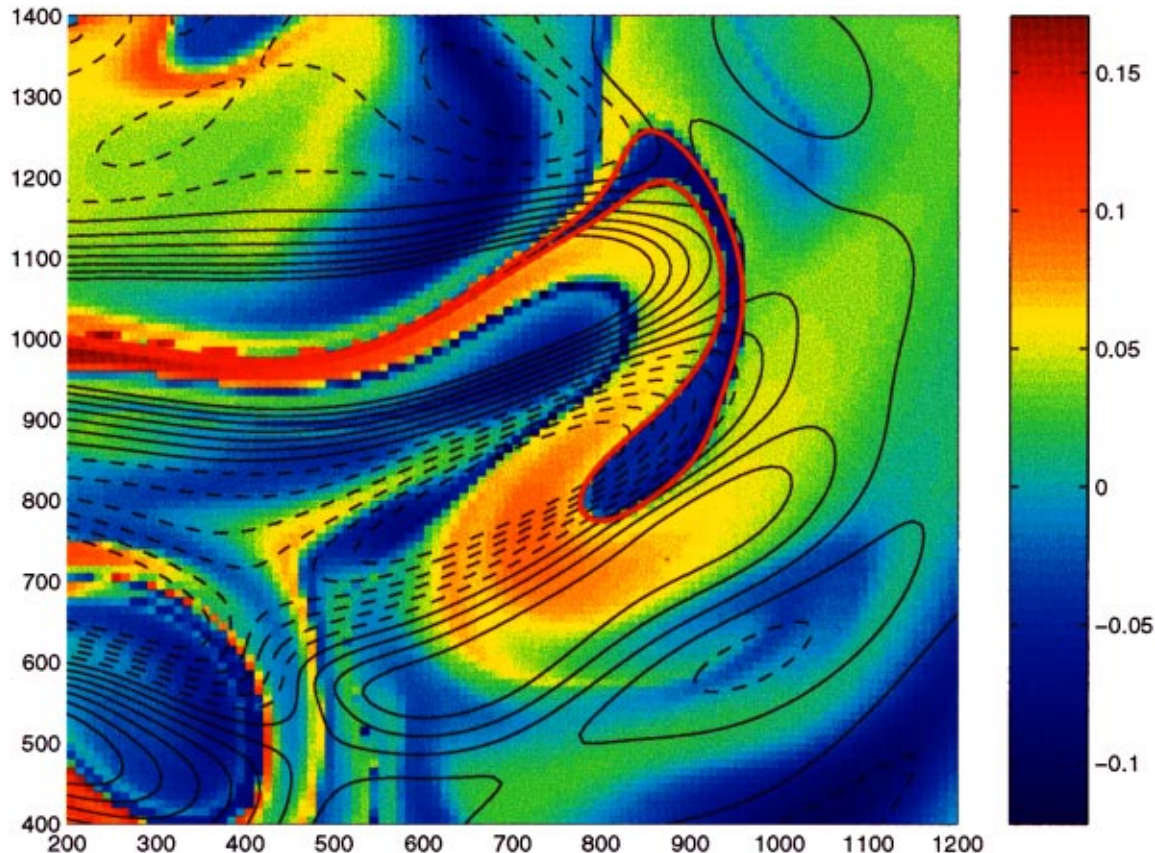

FIG. 2. Double-gyre primitive equations: stable manifold (bold red line) and patchiness plot of the x component of Lagrangian velocity, averaged over 60 days. The Eulerian velocity, averaged over the same 60-day interval, is shown contoured. Contour interval 0.05 m/s, $(\bar{u}_{min}, \bar{u}_{max}) = (-0.3 \text{ m/s}, 0.3 \text{ m/s})$

average f^* are invariant sets for the dynamics. Moreover, the joint level sets of time averages f_i^* of a system of orthogonal basis functions f_i can be shown to be invariant sets on which the dynamics of the flow is ergodic. These results rely on the use of Birkhoff's ergodic theorem.[15] For flows with aperiodic time dependence, the limit in question might not exist,[16] but the finite-time average plots still indicate a great deal about mixing properties of the flow, especially if the function f is chosen in a physically relevant way. The physical quantity that determines the statistical behavior of particle paths is the velocity that a particle samples along its path. The velocity vector $\mathbf{v}$ determines two functions: $v_x : \mathcal{M} \rightarrow \mathbb{R}$ and $v_y : \mathcal{M} \rightarrow \mathbb{R}$. Thus, we consider the finite-time average velocities $v_x^*(t, x_0, y_0) = [x(t, x_0, y_0) - x_0]/t$ and $v_y^*(t, x_0, y_0) = [y(t, x_0, y_0) - y_0]/t$, where $[x(t, x_0, y_0), y(t, x_0, y_0)]$ is the position at time t of a particle starting at (x_0, y_0) at time $t = 0$. Plots of $v_x^*(t, x_0, y_0)$ and $v_y^*(t, x_0, y_0)$ as functions of the initial particle locations, x_0, y_0 have been named *patchiness* plots by Malhotra *et al.*[9] after previous work by Pasmanter.[17]

IV. RESULTS

The above ideas are evaluated in the context of an eddy-resolving, reduced gravity, primitive equation model of the wind-driven circulation in an ocean basin. In brief, the shallow water equations,

$$\frac{\partial u}{\partial t} + u\frac{\partial u}{\partial u} + v\frac{\partial u}{\partial y} - f_0(1 + \beta y)v = -g'\frac{\partial h}{\partial x} + F^u + \nu\nabla^2 u,$$

$$\frac{\partial v}{\partial t} + u\frac{\partial v}{\partial x} + v\frac{\partial v}{\partial y} + f_0(1 + \beta y)u = -g'\frac{\partial h}{\partial y} + F^v + \nu\nabla^2 v,$$

$$\frac{\partial h}{\partial t} + \frac{\partial(uh)}{\partial x} + \frac{\partial(vh)}{\partial y} = 0,$$

are solved on a regular grid, $\Delta x = \Delta y = 10$ km using second-order finite difference methods.[18] The effects of smaller-scale motions have been subsumed in the Laplacian diffusion terms with an ''eddy viscosity'' coefficient ν; g' is the reduced gravity, i.e., the normal gravitational acceleration weighted by the density difference between the active upper layer and the quiescent lower layer $\Delta\rho/\rho$. No-slip boundary conditions are imposed on the velocities at the sidewalls. The parameter values are typical of basin scale simulations (see, e.g., Figueroa and Olsen[19]) and are given in Poje and Haller.[11]

The imposed wind stress, $(F^x, F^v) = [(\tau_0/\rho H_0) \times \sin(2\pi y/L_y), 0]$, sets up a double gyre circulation; a cyclonic (counterclockwise) circulation in the north and an anticyclonic circulation in the south. We concentrate our attention on the strong jet region that separates the two gyres. This jet is unstable and, like the midlatitude oceanic jets, it is meant to model, intermittently rolls up, shedding large-scale eddies in the process. A complete description of the finite-time-invariant manifold structure produced by transient hyperbolic points in the detaching eddy flow is given in Poje
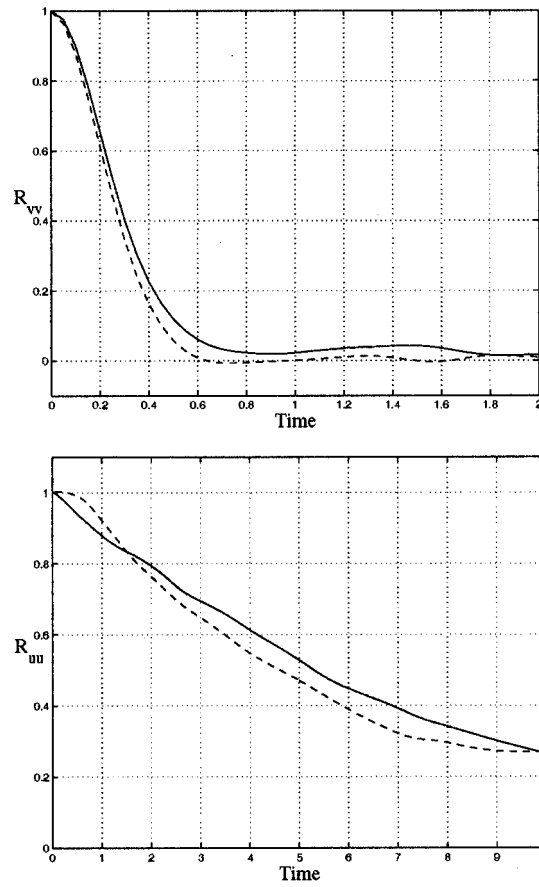

FIG. 3. The Lagrangian (upper) and Eulerian (lower) velocity autocorrelation functions in barotropic turbulence. In each, the autocorrelation of the y component of velocity is dashed; the x component is solid.

and Haller.[11] Here we concentrate on the relationship between such structures and Lagrangian statistical measures described by patchiness plots.

Figure 2 shows the intersection, at time $t = t_0$, of the finite-time stable manifold corresponding to a detaching meander event with the $x - y$ plane. The associated hyperbolic trajectory is located at $\Gamma \approx (950, 950)$. The Lagrangian manifold structure is superimposed on a patchiness plot of the 60-day averaged, x component of the velocity. The calculation was performed using 10 000 particles initialized on a regular grid at time t_0. The average velocity of each particle is computed and plotted at the initial particle location. The correspondence between the manifold geometry and the Lagrangian-averaged velocity is striking. The ''mixing channel'' formed by the extended branches of stable manifold clearly marks those initial conditions in the jet region that possess significantly negative average velocity. A contour plot of the x component of the Eulerian velocity, averaged over the same 60-day time period is also shown. While there is a strong correlation between the finite-time manifold geometry and spatial variations of the Lagrangian velocity statistics, there is very little correlation between the Eulerian and Lagrangian statistical descriptions on the time scales considered. The appearance of relatively long-lived coherent structures such as the detaching eddy implies that the dynamics of fluid particles, and hence Lagrangian statistics, are
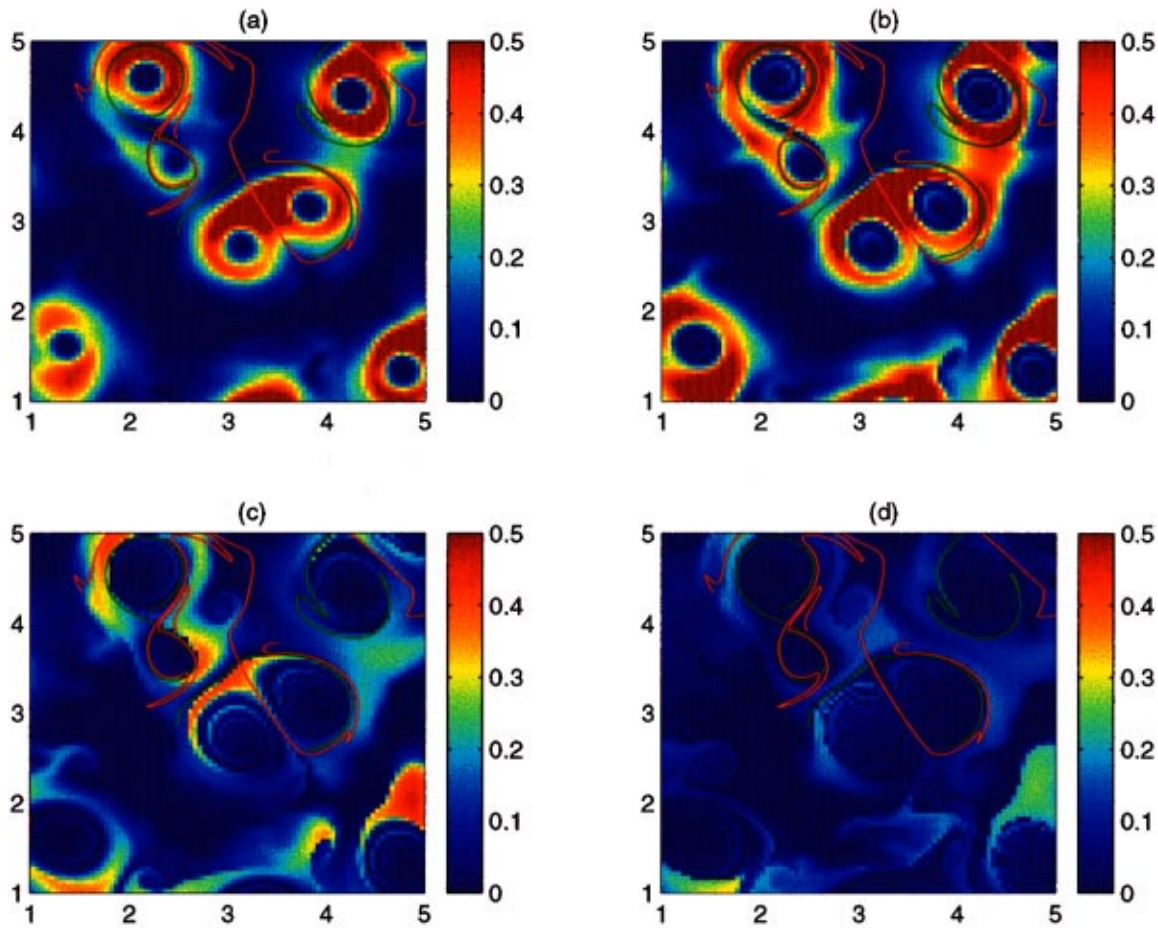
FIG. 4. Barotropic turbulence: patchiness plot of the magnitude of the Lagrangian-averaged velocity for averaging times (a) 0.5, (b) 1.0, (c) 2.5, and (d) 5.0. The stable (green) and unstable (red) finite time manifolds associated with three hyperbolic trajectories are superimposed.

dominated by the saddle dynamics associated with distinguished hyperbolic trajectories. Such structures point to strong spatial inhomogeneities in the flow and in the intermediate time Lagrangian statistics.

In order to test the persistence of such observations in less obviously well-ordered flow fields containing identifiable coherent structures, we consider the Lagrangian dynamics of freely decaying barotropic turbulence. The numerical model used is a standard spectral scheme (see Babiano *et al.*[3]) with 128^2 resolution on a scaled, $2\pi \times 2\pi$ domain solving the quasigeostrophic vorticity equation,

$$\frac{\partial q}{\partial t} + J(q, \psi) = \nu_4 \nabla^4 q,$$

where $q = (\nabla^2 - F^2)\psi$ and $F = 10$ is the scaled inverse of the Rossby deformation radius. The finite deformation radius decreases vortex–vortex interactions at scales greater than L/F and leads to the formation of relatively long-lived and robust vortex structures on this scale (see Provenzale *et al.*[20]).

The trajectories of 81^2, uniformly seeded particles are computed alongside the evolving velocity field. The Lagrangian and Eulerian velocity autocorrelations, defined by

$$R_{vv}(t, t_0) = \frac{\langle \mathbf{v}(t_0, \mathbf{x}_0) \cdot \mathbf{v}(t_0 + t, \mathbf{x}_0) \rangle}{\langle |\mathbf{v}(t_0, \mathbf{x}_0)|^2 \rangle}$$

and

$$R_{uu}(t, t_0) = \frac{\overline{\mathbf{u}(\mathbf{x}, t_0) \cdot \mathbf{u}(\mathbf{x}, t_0 + t)}}{\overline{|\mathbf{u}(\mathbf{x}, t_0)|^2}},$$

respectively, are shown in Fig. 3. Here the Lagrangian velocity along a trajectory, as a function of the initial position $\mathbf{x}_0$, is denoted by $\mathbf{v}(t, \mathbf{x}_0)$, while the Eulerian velocity field is denoted by $\mathbf{u}(\mathbf{x}, t)$. The operators $\langle (\cdot) \rangle$ and $\overline{(\cdot)}$ correspond to averaging over all initial conditions and all space, respectively. The autocorrelation times, given by

$$T_{\alpha\alpha}(t_0) = \int_0^\infty R_{\alpha\alpha}(t, t_0) dt,$$

are different for the two processes with the Lagrangian time scale, $T_{vv} \approx 0.5$, considerably shorter than the Eulerian, $T_{uu} \approx 8$. The difference between the two time scales can be explained by the presence of robust coherent vortex structures that evolve relatively slowly in the Eulerian frame while effectively mixing Lagrangian particles. These are the conditions under which the analytic conditions for the existence of finite-time-invariant manifolds are satisfied (see Haller and Poje[10]), and the existence of organizing finite-time manifolds can be concluded.
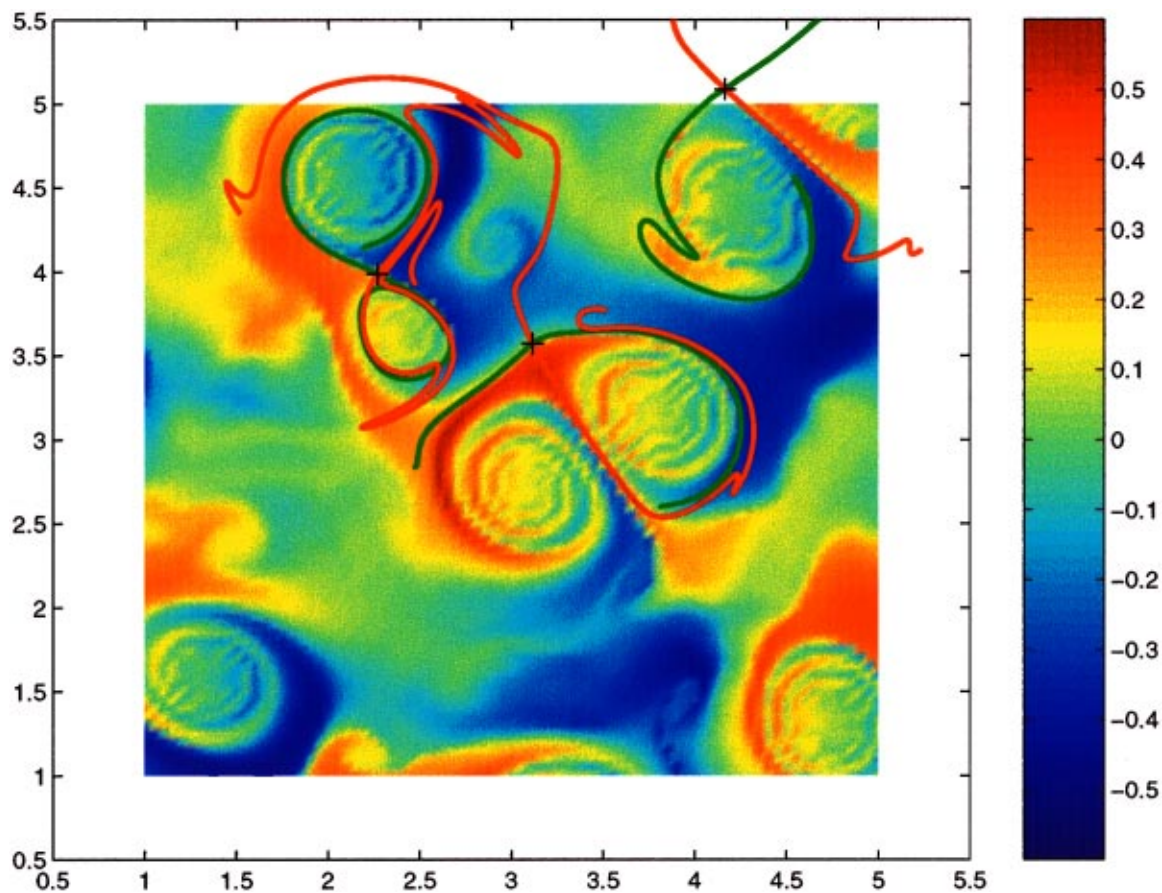
FIG. 5. Barotropic turbulence: patchiness plot of the x component of Lagrangian velocity, averaged over 2.5 time units with finite time manifolds superimposed. Unstable, W^u, in red. Stable, W^s in green. The three hyperbolic points are marked by crosses, $+$.
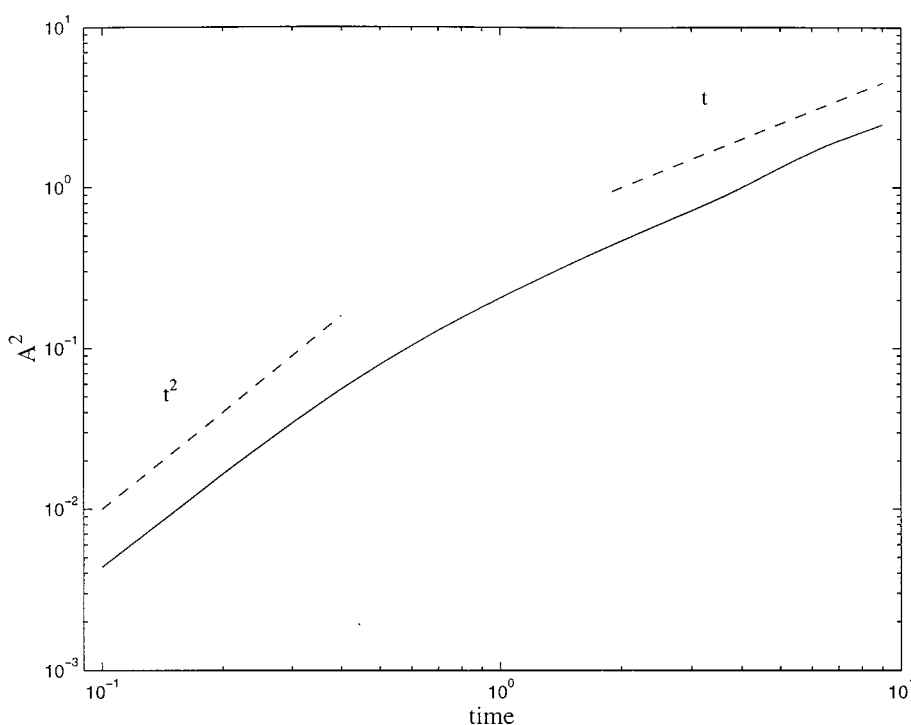

FIG. 6. The absolute dispersion curve for the barotropic turbulence field.

Figure 4 shows the finite-time stable and unstable manifolds computed for a subset of three hyperbolic trajectories corresponding to two pairs of like-signed vortices and a vortex dipole. From the geometric dynamical systems standpoint, the hyperbolic trajectories associated with rotating pairs of like-signed vortices are the most robust features of the flow existing for extremely long times ($t > 40$) with time-averaged hyperbolicity $\lambda \sim 1.4$. Conversely, the propagating dipoles do not produce an easily identified frozen-time stagnation point in the fixed reference frame. The hyperbolic trajectories associated with the dipole structure are, in this case, shorter lived ($t < 10$) with weaker averaged hyperbolicity, $\lambda \sim 0.8$.

Superimposed on the manifold geometry are patchiness plots of the magnitude of the averaged Lagrangian velocity, $\langle |\mathbf{v}| \rangle = \langle (\mathbf{v} \cdot \mathbf{v})^{1/2} \rangle$ for four different averaging times. At early times, significant Lagrangian-averaged velocities are confined to the high-swirl regions in the interior of the vortices. After a few eddy-turnover times ($t = 2.5$), the Lagrangian average velocity in the vortex cores, as defined by the manifolds, is zero. Appreciable velocities are concentrated near the hyperbolic points and in the mixing regions straddling the manifolds. In Fig. 5, the close relation between the finite-time manifold geometry and changes in the sign of the x component of the Lagrangian average velocity is clearly shown for an intermediate averaging time. The use of edge detection in patchiness plots to determine the finite-time manifold geometry has recently been proposed by Bowman[21] in the context of atmospheric mixing problems.

We note that as the averaging time is increased, the spatial structure in the patchiness plots is lost. For times longer than several Lagrangian velocity autocorrelation times, individual particles see the entire spectrum of velocities and the average velocity is zero. For intermediate time scales, which may in the geophysical context be the time scales of observation and interest, dispersion statistics are not amenable to Taylor analysis in the diffusion limit and typically show anomalous dispersion rates (see Fig. 6). From the results shown here, it appears reasonable to conclude that in a variety of flows, particle dynamics on intermediate time scales are dominated by the presence of finite-time Lagrangian structures associated with distinguished hyperbolic trajectories. The exact, qualitative relationship between intermediate-time statistics and the presence of organizing geometric structures remains the focus of current research.

ACKNOWLEDGMENTS

[1] H. Aref, ''Stirring by chaotic advection,'' J. Fluid Mech. **143**, 1 (1984).

[2] J. M. Ottino, *The Kinematics of Mixing: Stretching, Chaos and Transport* (Cambridge University Press, Cambridge, 1989).

[3] A. Babiano, G. Bofetta, A. Provenzale, and A. Vulpiani, ''Chaotic advection in point vortex models and two-dimensional turbulence,'' Phys. Fluids **6**, 2465 (1994).

[4] D. DelCastillo-Negrete, ''Asymmetric transport and non-Gaussian statistics of passive scalars in vortices in shear,'' Phys. Fluids **10**, 576 (1998).

[5] J. B. Weiss, A. Provenzale, and J. C. McWilliams, ''Lagrangian dynamics in high-dimensional point vortex systems,'' Phys. Fluids **8**, 1929 (1998).

[6] G. M. Zaslavsky, ''Lagrangian turbulence and anomalous transport,'' Fluid Dyn. Res. **8**, 127 (1991).

[7] E. M. Ziemniak, C. Jung, and T. Tél, ''Tracer dynamics in open hydrodynamical flows as chaotic scattering,'' Physica D **44**, 123 (1994).

[8] I. Mezić, ''On geometrical and statistical properties of dynamical systems: Theory and applications,'' Ph.D. thesis, California Institute of Technology, 1994.

[9] N. Malhotra, I. Mezić, and S. Wiggins, ''Patchiness: A new diagnostic for Lagrangian trajectory analysis in time-dependent fluid flows,'' Int. J. Bifurcation Chaos Appl. Sci. Eng. **8**, 1053 (1998).

[10] G. Haller and A. C. Poje, ''Finite time transport in aperiodic flows,'' Physica D **119**, 352 (1998).

[11] A. C. Poje and G. Haller, ''Geometry of cross-stream mixing in a double-gyre ocean model,'' J. Phys. Oceanogr. **29**, 1649 (1999).

[12] P. D. Miller, C. K. R. T. Jones, A. M. Rogerson, and L. J. Pratt, ''Quantifying transport in numerically generated velocity fields,'' Physica D **101**, 1 (1997).

[13] J. Weiss, ''The dynamics of enstrophy transfer in 2-dimensional hydrodynamics,'' Physica D **48**, 273 (1991).

[14] I. Mezić and S. Wiggins, ''A method for visualization of invariant sets of dynamical systems based on the ergodic partition,'' Chaos. **9**, 213 (1999).

[15] K. Petersen, Ergodic Theory (Cambridge University Press, Cambridge, 1995).

[16] D. D'Allessandro, I. Mezić, and M. Dahleh, ''Some ergodic theorems for sequences of measure preserving transformations,'' UCSB preprint (1999).

[17] R. Pasmanter, ''Anomalous diffusion and patchiness generated by Lagrangian chaos in shallow tidal flows,'' Phys. Fluids A **3**, 1441 (1991).

[18] D. A. Jones, A. C. Poje, and L. G. Margolin, ''Resolution effects and enslaved finite difference schemes for a double gyre, shallow-water model,'' Theor. Comput. Fluid Dyn. **9**, 269 (1997).

[19] H. A. Figueroa and D. B. Olsen, ''Eddy resolution versus eddy diffusion in a double gyre GCM. Part I: The Lagrangian and Eulerian description,'' J. Phys. Oceanogr. **24**, 371 (1998).

[20] A. Provenzale, A. Babiano, and A. Zanella, ''Dynamics of Lagrangian tracers in barotropic turbulence,'' in *Mixing: Chaos and Turbulence,* Proceedings of a NATO Advanced Study Institute, Cargese, Corsica, 7–20 July 1996 (in press).

[21] K. P. Bowman, ''Manifold geometry and mixing in observed atmospheric flows,'' preprint, 1999.